Purification and characterization of a tungsten-containing formate dehydrogenase from Desulfovibrio gigas

ARTICLE *in* BIOCHEMISTRY · JANUARY 2000

Impact Factor: 3.02 · Source: PubMed

10 AUTHORS, INCLUDING:

Pedro Tavares
New University of Lisbon
75 PUBLICATIONS **1,462** CITATIONS
SEE PROFILE

Sergey A Bursakov
Spanish National Research Council
40 PUBLICATIONS **856** CITATIONS
SEE PROFILE

José J G Moura
New University of Lisbon
572 PUBLICATIONS **12,166** CITATIONS
SEE PROFILE

Isabel Moura
New University of Lisbon
228 PUBLICATIONS **5,907** CITATIONS
SEE PROFILE

Purification and Characterization of a Tungsten-Containing Formate Dehydrogenase from *Desulfovibrio gigas*†

Maria J. Almendra,‡ Carlos D. Brondino,‡ Olga Gavel,‡ Alice S. Pereira,‡ Pedro Tavares,‡,§ Sergey Bursakov,‡ Rui Duarte,‡ Jorge Caldeira,‡,|| Jose J. G. Moura,‡ and Isabel Moura*,‡

Departamento de Química (Centro de Química Fina e Biotecnologia), Faculdade de Ciências e Tecnologia, Universidade Nova de Lisboa, 2825-114 Caparica, Portugal, Instituto Superior de Ciências da Saúde -Sul, 2825-114 Caparica, Portugal, and Instituto Piaget, 2800 Almada, Portugal

Received January 12, 1999; Revised Manuscript Received September 8, 1999

ABSTRACT: An air-stable formate dehydrogenase (FDH), an enzyme that catalyzes the oxidation of formate to carbon dioxide, was purified from the sulfate reducing organism *Desulfovibrio gigas* (*D. gigas*) NCIB 9332. *D. gigas* FDH is a heterodimeric protein [α (92 kDa) and β (29 kDa) subunits] and contains 7 ± 1 Fe/protein and 0.9 ± 0.1 W/protein. Selenium was not detected. The UV/visible absorption spectrum of *D. gigas* FDH is typical of an iron−sulfur protein. Analysis of pterin nucleotides yielded a content of 1.3 ± 0.1 guanine monophosphate/mol of enzyme, which suggests a tungsten coordination with two molybdopterin guanine dinucleotide cofactors. Both Mössbauer spectroscopy performed on *D. gigas* FDH grown in a medium enriched with ^{57}Fe and EPR studies performed in the native and fully reduced state of the protein confirmed the presence of two [4Fe-4S] clusters. Variable-temperature EPR studies showed the presence of two signals compatible with an atom in a d^1 configuration albeit with an unusual relaxation behavior as compared to the one generally observed for W(V) ions.

Molybdenum- and tungsten-containing enzymes are a wide group of proteins present in several living systems that participate in hydroxylation and oxo-transfer reactions in which the metal ion cycles between the oxidation states VI and IV (*1*−*3*). With the exception of nitrogenase, in these proteins the metal ion is usually associated with one or two pterin derivatives that form a metallic cofactor. Also, these proteins may have in addition other cofactors such as iron−sulfur centers, flavin, and hemes which are assumed to be involved in intramolecular electron-transfer processes. Most of the proteins of the bacterial organisms studied so far contain molybdenum in their active sites, but in the last 2 years the number of proteins that incorporate tungsten has considerably increased (*2*). However, the role of tungsten seems secondary in the bacterial metabolism, since for most of the known tungstoenzymes there is an analogue molybdoenzyme performing the same function within the same organism. The only exception to this rule is the hyperthermophilic archaea whose growth is W-dependent and is incapable of utilizing molybdenum (*4, 5*).

Formate dehydrogenases (FDHs)[1] are a diverse group of enzymes found in both prokaryotes and eukaryotes which catalyze the reversible two-electron oxidation of formate to carbon dioxide. Recently, the first crystal structure of a molybdenum-containing FDH from *E. coli* has been reported (*6*). The metal ion in this enzyme is coordinated by two MGD cofactors and by a selenocysteine ligand. We have reported the biochemical and spectroscopic characterization of a Mo-containing FDH from the sulfate reducer *D. desulfuricans* ATCC 27774 (*7*). The results obtained for the *D. desulfuricans* FDH indicate that the metal ion is coordinated by two MGD and Se such as in *E. coli* FDH. Recent results obtained in the *E. coli* Mo-FDH indicate that this enzyme catalyzes formate oxidation without oxygen transfer (*8*), and EXAFS studies showed the presence of a potentially redox-active seleno-sulfide ligand (*9*). Furthermore, EXAFS studies performed in the *D. desulfuricans* Mo-FDH suggested a non-metal-based redox chemistry in a molybdoenzyme (*10*). These results seem to indicate that most likely the Se-containing Mo-FDHs may have a different catalytic mechanism from that generally proposed for the Mo- and W-containing proteins. FDHs from anaerobic microorganisms are typically Mo-containing enzymes (*11, 12*), but there are a number of reports of W-FDHs partially purified (*2*). However, the Se-containing FDH from *C. thermoaceticum*, the first W-containing enzyme to be purified, is to date the only W-FDH well characterized both biochemically and spectroscopically (*13, 14*). Although the field of the tungstoenzymes is still in its beginning (*2*), future comparative studies performed in Se- and non-Se-coordinated Mo- and W-FDHs are necessary in order to elucidate the differences and common aspects of the general catalytic mechanism(s).

† This work was supported by Grants PRAXIS 2/2.2/QUI/3/94 (I.M.), PRAXIS 2/2.1/BIO/05/94 (J.J.G.M.), BPD/14146/97, BPD/16362/98, BD/137775/97, and BD/9042/96.

* To whom correspondence should be addressed. E-mail: isa@dq.fct.unl.pt. Fax: 351-1-2948550.

‡ Universidade Nova de Lisboa.

§ Instituto Piaget.

|| Instituto Superior de Ciências da Saúde -Sul.

[1] Abbreviations: FDH, formate dehydrogenase; *E., Escherichia*; MGD, molybdopterin guanine dinucleotide; *D., Desulfovibrio*; EXAFS, extended X-ray absorption fine structure; *C., Clostridium*; SRB, sulfate reducing bacteria; ADH, aldehyde dehydrogenase; EPR, electron paramagnetic resonance; HPLC, high-pressure liquid chromatography; TPTZ, 2,4,6-tris(2-pyridyl)-1,3,5-triazine; AOR, aldehyde oxidoreductase.

10.1021/bi990069n CCC: $18.00
Published on Web 11/12/1999

To our knowledge, there are only two reports on FDH isolated from SRB (*7, 15*). Also, all the studies performed in SRB indicate that these organisms prefer molybdenum to tungsten. The only tungstoprotein reported in a sulfate reducing bacteria is, at present, the W-containing ADH isolated from *D. gigas*, which was obtained when the growth medium was supplemented with tungsten (*16*).

In this paper we report the biochemical and spectroscopic characterization of a W-containing FDH obtained from the sulfate-reducer *D. gigas*. This enzyme was partially purified by Riederer-Henderson and Peck (*17*). These authors proposed a periplasmatic localization for this protein. FDHs from anaerobes are very sensitive to oxygen. However, FDH from both *D. gigas* and *D. desulfuricans* (*7*) does not lose activity in the presence of air and therefore can be easily manipulated. EPR and Mössbauer studies performed on samples of *D. gigas* FDH showed the presence of two different iron−sulfur clusters. Also, variable-temperature EPR studies showed the presence of a typical signal of W(V) albeit with an unusual relaxation behavior. These results are discussed in comparison with the results obtained in other related proteins.

MATERIALS AND METHODS

Organisms and Growth Conditions. *D. gigas* NCIB 9332 cells were grown at 37 °C in a lactate−sulfate medium, under anaerobic conditions as described elsewhere (*18*).

Protein Purification. A cell-free extract (soluble extract) was obtained after cell disruption using a French−Gaulin homogeneizer and centrifugation (Sigma 3 K 30 centrifuge, and a 12 156 rotor) at 10 000 rpm for 30 min. Afterward, ultracentrifugation (Beckman L-70 ultracentrifuge, 45 Ti rotor) at 42 000 rpm for 90 min was made, to separate the membranes. All these steps were performed at 4 °C. This extract was kept at −70 °C until use.

The soluble extract (2200 mL) was loaded onto an anion exchange column (DEAE 52 cellulose, Whatman 6 × 32.5 cm) equilibrated with 10 mM Tris-HCl buffer (pH 7). A linear gradient (0.01−0.5 M) was applied with a total volume of 2 L. The enzyme (specific activity = 1.1 units·mg^{-1}) was found in the fraction eluted at 200 mM Tris-HCl (pH 7). This fraction was then dialyzed against 10 mM Tris-HCl buffer (pH 7) and applied to an anion exchange column (Source 15, Pharmacia, 2.7 × 20 cm). The proteins were eluted using a Tris-HCl (pH 7) buffer gradient (0.01−0.50 M); the fraction that mainly contained FDH activity was collected at 200 mM ionic strength. The ionic strength was decreased by adding Millipore water. The next step was a gel filtration column (Superdex 200, Pharmacia, 2.7 × 100 cm) equilibrated with 300 mM Tris-HCl buffer (pH 7). The specific activity in the best fraction of FDH after this step was 11.8 units·mg^{-1}. After dialysis, the final step was performed again on a Source 15 column (2.7 × 20 cm), using a Tris-HCl buffer (pH 7) gradient (0.01−0.5 M). After this step, the enzyme was found to be pure (specific activity = 34.1 units·mg^{-1}, Table 1).

D. gigas FDH Grown in a Medium Enriched with ^{57}Fe. A parallel study was developed with FDH from *D. gigas* NCIB 9332 cells, grown anaerobically in a basic lactate−sulfate medium (*18*) enriched with ^{57}Fe. The purification was performed in a similar way as the one previously described.

Activity Assays. The formate dehydrogenase assay was performed with formate as the substrate and benzyl viologen as the electron acceptor. A standard optical assay of formate dehydrogenase was performed at room temperature under argon atmosphere, by monitoring the benzyl viologen reduction at 555 nm (ϵ = 12 mM^{-1} cm^{-1}) as described by Costa et al. (*7*).

The reaction mixture contained, in a final volume of 1 mL, 50 mM Tris-HCl buffer (pH 8), 10 mM sodium formate, 0.3 mM benzyl viologen, 100 mM β-mercaptoethanol, and an appropriate amount of enzyme. All reagents were flushed with argon before use in the reaction mixture. Initially, the enzyme was incubated under an argon atmosphere for 10 min with Tris-HCl buffer (pH 8). Then, keeping an argon atmosphere, β-mercaptoethanol and benzyl viologen were added. The reaction was started by the anaerobic addition of sodium formate. Blanks were done with the same reaction mixture, excluding the substrate sodium formate. All spectrophotometric analysis was performed on a Shimadzu UV-2101 PC spectrophotometer. One unit of FDH activity was defined as the amount of enzyme catalyzing the reduction of 2 μmol of benzyl viologen/min.

UV/Visible Measurements. The UV/visible optical spectrum of the as-isolated enzyme was recorded on a Shimadzu UV-2101 PC split-beam spectrophotometer using 1 cm quartz cells.

Molecular Mass Determination. The molecular mass of the purified protein was determined by gel filtration chromatography using a Superdex 200 column 10/30 HR (Pharmacia) connected to an HPLC system (Jasco PU-980). The elution buffer was 100 mM Tris-HCl (pH 7.6) containing 150 mM NaCl, and the proteins used as size markers were ribonuclease A (13.7 kDa), chymotrypsinogen A (25 kDa), ovalbumin (43 kDa), bovine serum albumin (67 kDa), aldolase (158 kDa), catalase (232 kDa), and ferritin (440 kDa) from Pharmacia Biotech. Subunit composition was determined by SDS−PAGE at 12.5% using the Pharmacia Low Molecular Mass Kit as standard for calibration.

Protein and Metal Quantification. Bradford (*19*) and Lowry (*20*) methods were used for estimation of the protein concentration, with bovine serum albumin as a standard. Concentrations of pure enzyme samples were monitored spectrophotometrically. The quantification of tungsten and iron was performed by inductively coupled plasma emission analysis. Iron determination was also performed by the TPTZ method.

pH Dependence of the Enzymatic Activity. The pH dependence of the enzymatic activity was measured at 50 mM ionic strength with the pH ranging from 5.5 to 10, using citric acid/potassium phosphate, Tris-HCl, and glycine/NaOH buffer systems.

Analysis of Pterin Nucleotides. Nucleotides were extracted from *D. gigas* FDH by a previously published procedure (*21*). Cofactor extraction was performed with sulfuric acid (3% v/v) for 10 min at 95 °C, with subsequent centrifugation in a microcentrifuge for 5 min at 10 000 rpm. Chromatography analysis was done using a Merck L-7100 HPLC equipped with an UV detector L-7100 and D-7000 computer interface. Hydrolyzed nucleotide peak areas were quantified at 254 nm. Ammonium acetate (HPLC grade), 50 mM, pH 6.8, was used as eluent at a flow rate of 1 mL min^{-1}, using a Merck LiChorspher 100 (250 × 4) RP-18e, 4 μm column. Quantitative determinations were done with an injection loop volume

Table 1: Purification of *D. gigas* FDH

purification step	volume (mL)	total protein (mg)	total units (U)	sp act. (U/mg)	yield (%)
soluble extract	2200	80660	8001	0.0992	−
DEAE-52	850	25075	27220	1.086	100
Source 15	500	885	9047	10.22	33
Superdex 200	160	165	1944	11.8	7
Source 15	44	28.5	973	34.1	4

of 50 μL from extracted nucleotides and fresh solutions of mononucleotides (Sigma) submitted to identical acid/heating treatment.

Mössbauer Spectroscopy. The weak-field Mössbauer spectrometer is of the constant-acceleration type and is equipped with a Janis 8DT variable-temperature cryostat. The zero velocity of the Mössbauer spectrum is referred to the centroid of the room-temperature spectrum of a metallic iron foil.

EPR Spectroscopy. Variable-temperature EPR measurements at X-band were performed on a Bruker EMX spectrometer equipped with a dual-mode cavity (Model ER 4116DM) and an Oxford Instruments continuous flow cryostat. EPR spectra were simulated using the program WIN-EPR simfonia V.1.2 from Bruker Instruments, Inc. The signals associated with each paramagnetic center were separately simulated, normalized by double integration, and then added altogether in different proportions until good agreement was obtained between experimental and simulated data.

RESULTS AND DISCUSSION

Purification and Localization of Formate Dehydrogenase. The early observation that the *D. gigas* FDH activity in soluble extract was air-insensitive made the enzyme purification easier (*17*). This contrasts with the reports that most FDHs isolated from anaerobes lose activity when stored aerobically and thus must be purified under strictly anaerobic conditions. *D. gigas* FDHs have been purified to a specific activity of 34 units/mg of protein. A summary of the purification scheme of *D. gigas* FDH is given in Table 1.

Molecular Mass and Metal Content. The molecular mass of the native enzyme was determined by gel filtration chromatography. A single symmetrical elution peak was detected corresponding to a molecular mass of 120 ± 2 kDa. Under denaturing conditions (SDS−PAGE), two bands were observed on the gel with estimated molecular masses of 92 and 29 kDa (Supporting Information). Apparently, formate dehydrogenase is a heterodimeric protein which contains two types of subunits ($\alpha\beta$). No hemes *c* were detected when a specific gel staining was performed. Non-heme iron was detected either by the TPTZ method or by plasma emission. Metal quantification revealed the presence of 7 ± 1 Fe/protein (TPTZ and plasma emission) and 0.9 ± 0.1 W/protein (plasma emission). Selenium was not detected.

Enzymatic Properties. D. gigas FDH is isolated in the presence of oxygen and can be stored aerobically. The determination of the enzymatic activity depends critically upon the anaerobic conditions of the assay; the presence of β-mercaptoethanol is required, which has already been reported (*17*). The role of the thiol in the activation of FDH is still unclear, although it is probably needed to remove

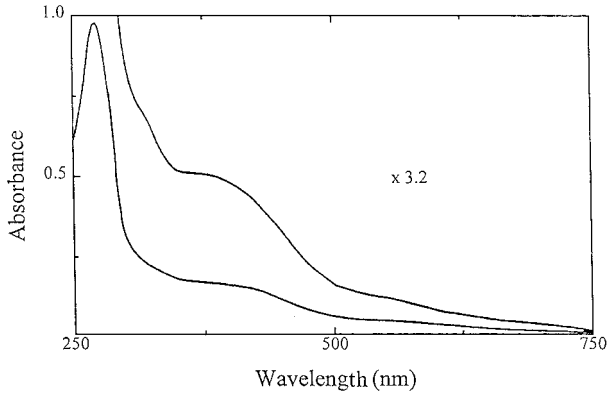

FIGURE 1: UV−visible absorption spectrum of as-purified *D. gigas* FDH.

oxygen and also to lower the redox potential of the assay system. In its presence, a small lag phase is detected. Small amounts of oxygen in the enzymatic assay dramatically inhibited the enzymatic reaction.

The enzyme exhibits an optimal activity at pH 8 in Tris-HCl buffer, with a sharp decrease above pH 8.5. Below pH 6.5, the enzyme was practically inactive (Supporting Information).

The UV/visible absorption spectrum of *D. gigas* FDH (Figure 1) is typical of an iron−sulfur protein (*22*). The spectrum exhibits a shoulder at 320 nm and a broad absorbance band in the 400 nm spectral region. The absorption coefficient at 400 nm is 31 200 ± 2000 M^{-1} cm^{-1}, which suggests the presence of two [4Fe-4S] clusters per molecule of enzyme, assuming that the $\epsilon_{M,400\ nm}$ of one [4Fe-4S]-type cluster is approximately 16 000 M^{-1} cm^{-1}.

Analysis of Pterin Nucleotides. The quantitative analysis of extracted nucleotides from *D. gigas* FDH yielded a content of 1.3 guanine monophosphates per mole of enzyme (two determinations of the same protein batch) using area comparison of peaks with identical retention times (11.5 ± 0.3 min) measured at 254 nm. This analytical procedure is known to underestimate the nucleotide content, and as a consequence, because an integer value is expected the number 2 seems most reasonable. A W-coordination with two MGD cofactors per tungsten atom is proposed. This determination depends on the yield of the extraction−purification procedure (see Materials and Methods). Similar values have been obtained for other two-pterin-containing proteins where the metal atom is linked to two MGD cofactors (*9, 23*).

Mössbauer Studies. Figure 2 shows the Mössbauer spectra of the as-isolated (A) and formate-reduced (B) *D. gigas* FDH recorded at 4.2 K with a 50 mT magnetic field applied parallel to the γ-beam. The low-temperature, low-field spectrum of *D. gigas* FDH in the as-isolated form is a broad quadrupole doublet with an apparent quadruple splitting (ΔE_Q) of ≈1 mm/s and an isomer shift (δ) of 0.43 mm/s. A shoulder is observed at the inner part of the spectrum. The spectrum can be least-squares-fitted with four quadrupole doublets of equal intensity. The parameters obtained from this analysis (δ = 0.46, 0.44, 0.44, 0.38 mm/s and ΔE_Q = 1.43, 0.85, 1.28, 0.66, respectively) are typical of $[4Fe\text{-}4S]^{2+}$ clusters.

Reduction of the sample originates the appearance of a magnetic spectrum extending from −1.8 mm/s to 2.5 mm/s. This spectrum is similar to the one observed for the reduced

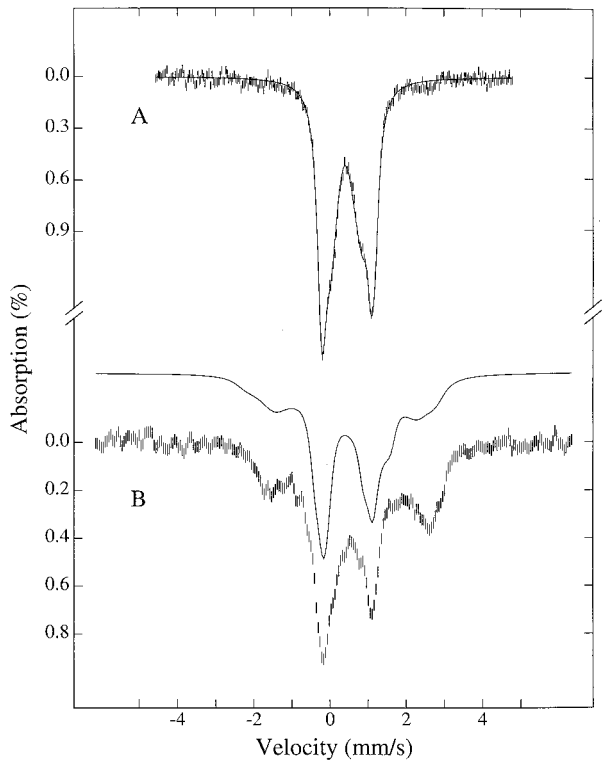

FIGURE 2: 4.2 K Mössbauer spectra of as-isolated (A) and fully formate-reduced (B) ^{57}Fe-enriched *D. gigas* FDH. Both spectra were recorded with a field of 50 mT applied parallel to the direction of γ-radiation. The solid line in spectrum A is a least-squares fit of four quadrupole doublets to the data (see text). The solid line at top of spectrum B is a theoretical simulation of the spectrum of the [4Fe-4S] clusters in *D. desulfuricans* FDH (*7*) recorded under the same experimental conditions as in spectrum B.

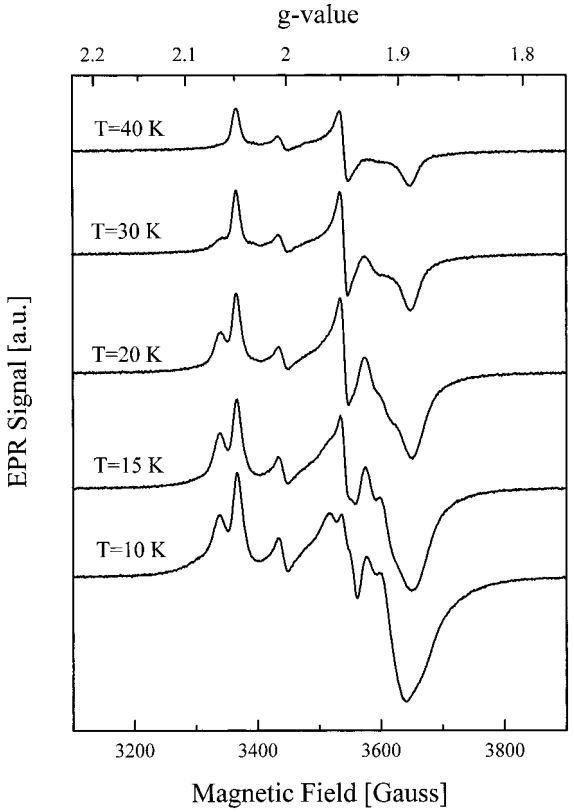

FIGURE 3: Variable-temperature EPR spectra taken in the fully formate-reduced state of *D. gigas* FDH. Experimental conditions: microwave power, 2 mW; modulation amplitude, 4 G_{pp}; microwave frequency, 9.65 GHz.

D. desulfuricans FDH (*7*). *D. desulfuricans* FDH is a complex protein that contains *c*-type heme groups, a molybdenum−pterin site, and two [4Fe-4S]$^{+2/+1}$, one of them displaying unusually small hyperfine coupling constants in the reduced state. For comparison, a theoretical simulation of the [4Fe-4S]$^{+1}$ clusters in *D. desulfuricans* FDH is plotted on top of Figure 2B. The Mössbauer data in combination with the determined iron content suggest the presence of two [4Fe-4S] clusters in *D. gigas* FDH, such as in the *D. desulfuricans* protein. These results are supported by the following EPR data.

EPR Studies. In the as-isolated state, FDH displays an almost isotropic signal detectable at temperatures below 30 K that accounts for less than 0.1 spin/protein (data not shown). The addition of potassium ferricyanide did not produce significant changes in the intensity and shape of this signal. The EPR parameters ($g_1 = 2.001$, $g_2 = g_3 = 2.018$), shape, and temperature dependence of this signal are consistent with those observed for [3Fe-4S]$^{+1}$ clusters. As we expected, the Mössbauer studies described above did not detect the presence of these centers due to their weak intensity, which suggests that they may be originated by partial oxidative degradation of [4Fe-4S] clusters (*24*).

Figure 3 shows variable-temperature EPR spectra of a formate-reduced *D. gigas* FDH sample. The fact that the protein can be directly reduced by formate indicates that the enzyme is in a catalytic-competent state. EPR spectra with similar shape and intensity were also obtained when the samples were reduced with sodium dithionite. As shown in Figure 3, the EPR spectra of *D. gigas* FDH are complex and suggest the superposition of several signals associated with paramagnetic species with different *g*-values and relaxation times. An almost isotropic component with no significant changes in shape and position was observed up to 120 K. This signal accounted for less than 0.1 spin/protein and has EPR parameters typical of a radical ($g = 2.003$, peak-to-peak line width = 16 G). As shown in Figure 1, the lack of a characteristic flavin UV/visible spectrum in *D. gigas* FDH excludes the possibility of a flavin radical. A similar signal observed in FDH from *C. pasteurianum* was suggested to arise from the pterin cofactor (*25*).

Table 2: *g*-Values[a] and Line Widths[b] (in Parentheses) Obtained by Simulation of the EPR Spectra in *D. gigas* FDH

	g_1	g_2	g_3
Fe/S I	1.890 (21)	1.947 (11)	2.048 (11)
Fe/S II	1.885 (30)	1.922 (20)	2.062 (22)
W(V)	1.877 (34)	1.907 (26)	1.942 (14)
center IV	1.945 (36)	1.945 (36)	2.025 (40)

[a] *g*-Values (±0.001). [b] Line widths in Gauss.

The spectra shown in Figure 3 exhibit, in agreement with the Mössbauer data, two EPR rhombic signals with *g*-values (Table 2) and relaxation behavior characteristics of iron−sulfur clusters in the +1 state designated as centers Fe/S I and Fe/S II, respectively. The EPR signals of center I shown in Figure 3 are sharp, but the center II signal starts broadening at temperatures near 30 K. Double integration of the spectra at 30 and 25 K (when the resonances of center II are fully sharp, but have minor contributions of other paramagnets, as we discuss below) gives invariably a value of ca. ~1.7

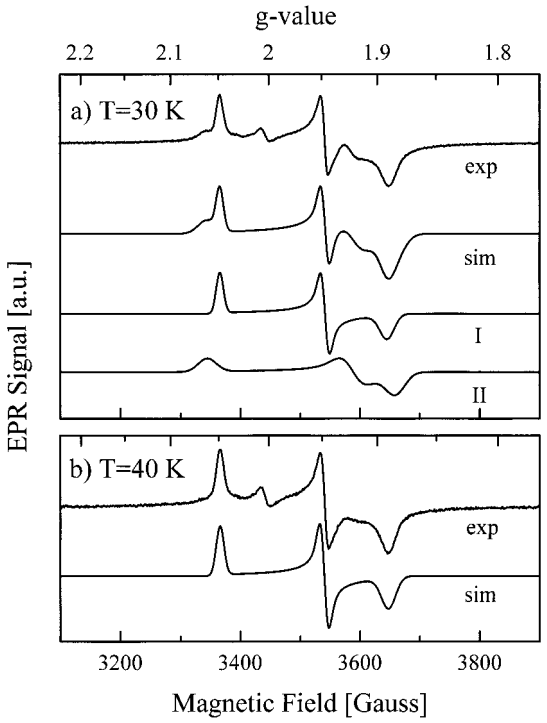

FIGURE 4: EPR spectra taken in the fully formate-reduced state of *D. gigas* FDH at 30 (a) and 40 K (b), together with spectral simulation. The EPR parameters used in the spectral simulation are given in Table 2. Experimental conditions as in Figure 3.

spin/protein. Simulation of the spectra at 30 K (Figure 4a) and 25 K (not shown) indicates a 1:1 stoichiometric ratio of both reduced Fe/S centers. These results are consistent with the observed Mössbauer data, suggesting also that the detected 7.4 ± 1 Fe/protein are arranged as two [4Fe-4S] clusters. Quantification of the apparent single rhombic signal observed at temperatures between 35 and 60 K (see, e.g., spectrum at 40 K in Figure 3) yielded spin concentrations between 1.6 and 1.3 spins/protein. As shown in Figure 4b, the simulation of these spectra assuming a single rhombic signal did not produce good agreement with the experimental spectrum, especially in the g_2 and g_3 spectral regions. These results indicate that broadened Fe/S II signals and/or other signals described below overlap with Fe/S I signals, even at the limit detection temperature of the Fe/S I signal (∼60−70 K).

Power-dependence experiments were also carried out with reduced *D. gigas* FDH samples at 25 K (Figure 5). The signal amplitudes of the low-field resonance (g_3) for both Fe/S signals were monitored as a function of increasing microwave power incident on the cavity. The experimental data were least-squares-fitted to the function: $S/\mathrm{sqrt}(P) \propto (1 + P/P_{1/2})^{b/2}$, where S is the signal amplitude, P is the microwave power incident on the cavity, $P_{1/2}$ is the microwave power at which the saturation factor is 0.5, and b is a constant characteristic of the broadening mechanism (*26*). The values obtained for $P_{1/2}$ (see caption to Figure 5) indicate that both iron−sulfur centers have approximately similar saturating behavior albeit with a different broadening mechanism as indicated by the different slopes at high values of P [b = 0.12(1) and 0.10(1) for Fe/S I and II, respectively]. Also, the line shape remains constant under non- and saturating conditions for both iron−sulfur centers (not shown). These characteristics are kept at temperatures below 20 K where

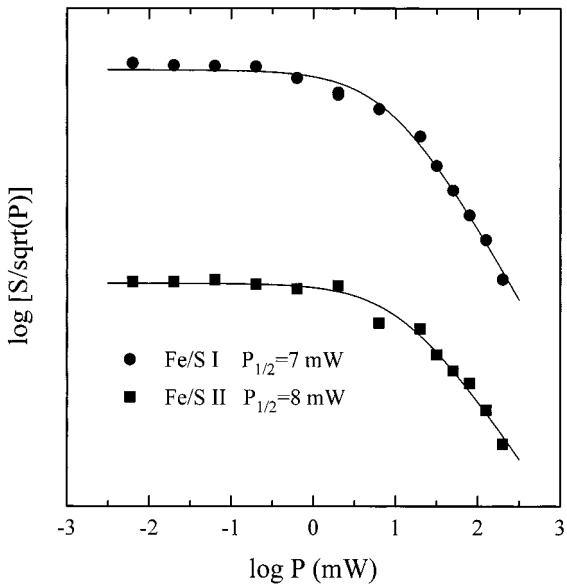

FIGURE 5: Microwave power saturation curves for the EPR signals of dithionite-reduced samples of *D. gigas* FDH at 25 K. The solid lines represent fits to the data, as explained in the text.

the iron−sulfur resonances are saturated even at very low microwave power. Although power-dependence studies are difficult to interpret due to the overlap of the iron−sulfur signals with other signals, the spectral simulation indicates, within experimental error, that both Fe/S signals keep the overall line shape.

D. gigas FDH at temperatures below 25 K exhibits other EPR signals that overlap with those of the iron−sulfur centers (Figure 3). Subtraction of the spectra in the 5−20 K temperature range, with different proportions of the spectra at higher temperatures, suggested the presence of two additional signals (hereafter designated as III and IV, respectively) both having an overall shape compatible with a spin $S = 1/2$. Simulation of the spectra between 5 and 20 K indicates an ∼1:1 stoichiometric ratio between the species giving signals III and IV and yielded the EPR parameters given in Table 2. Figure 6 shows the simulation of the spectrum at 10 K. As seen in Figure 3, it is evident that the decrease in temperature produces a concomitant increase in the intensity of signals III and IV when compared to those of the Fe/S signals. However, quantification of the signal at 10 K yielded a spin concentration lower than that for the spectra at 25 and 30 K. This indicates that the apparent increase of the III and IV signal intensities is produced by the saturation of the iron−sulfur resonances between 5 and 20 K. An estimation of the spin concentration for centers III and IV from the concentration evaluated for the signal at 10 K and the stoichiometric ratio among centers obtained by simulation yielded ∼0.3 spin/protein. Moreover, the EPR intensity of signals III and IV follows approximately a $1/T$ dependence with temperature (not shown), indicating that they are not saturated and, also, that they are produced by species with $S = 1/2$.

The g-values obtained for species III are consistent with an atom in a d^1 configuration. The spin concentration evaluated for center III is compatible with W(V) species in equilibrium with the EPR-silent W(IV) and W(VI) species. However, tungsten in a d^1 configuration shows in most cases hyperfine splitting with the ^{183}W nucleus ($I = 1/2$, 14.4%

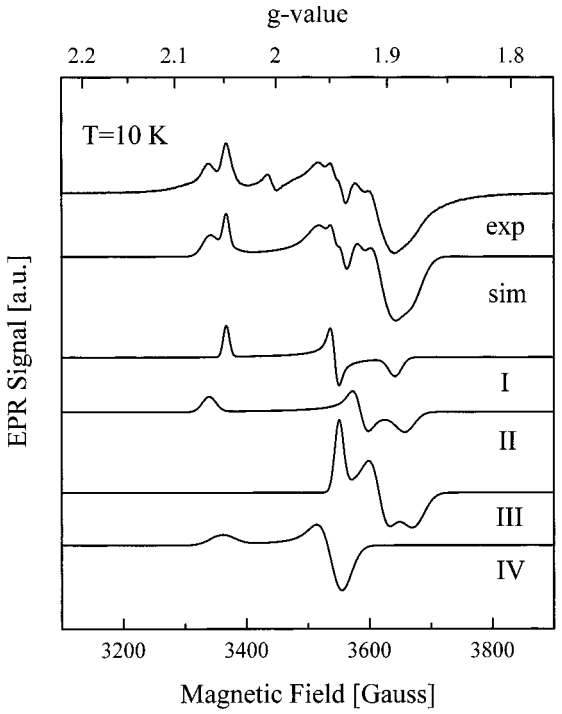

FIGURE 6: EPR spectra taken in the fully formate-reduced state of *D. gigas* FDH at 10 K, together with spectral simulation. The EPR parameters used in the spectral simulation are given in Table 2. Experimental conditions as in Figure 3.

natural abundance) and resonances observable at temperatures above 100 K. Hyperfine lines may be too difficult to be observed due to a complex overlap of multicomponents in this spectral region. However, there are cases reported where hyperfine lines of W(V) were not observed (*2*). Signal III is well detected at 25 K, and no broadening is observed from 10 to 25 K. This indicates a higher broadening temperature for signal III. Therefore, the lack of detection of the W signal at higher temperatures, but below 70 K (above 70 K no EPR signals were observed), is likely due to the overlap with the iron−sulfur resonances that masked the W signal. The undetection of EPR signals associated with W(V) at temperatures above 70 K indicates an unusual fast relaxation behavior for tungsten and suggests that W(V) is magnetically coupled to another faster relaxing paramagnet. Assuming that the broadening of the W resonances is produced at temperatures higher than 25 K, the enhancement of the relaxation properties of W(V) in *D. gigas* FDH may be due to the coupling of the tungsten atom with one of the iron−sulfur centers (*27*). These results are supported by studies performed recently on a FDH isolated from *D. alaskensis*, a closely related FDH to the *D. gigas* enzyme. EPR studies performed on this enzyme detected the broadening of W signals at ~70 K, apparently by magnetic coupling with the Fe/S I cluster (Brondino, C. D., Almendra, M. J., Feio, M. J., Caldeira, J., Moura, I., and Moura, J. J. G., in preparation). Studies performed on model systems suggest a correlation between the g_{av} and the number of thiolate ligands in oxo-tungsten (V) species (*28*). According to this correlation, the W center in *D. gigas* FDH ($g_{av} = 1.91$) should be linked to the two pterin cofactors of MGD type with one of the sulfur atoms weakly coordinated, as is the case for the molybdenum center in dimethyl sulfoxide reductase from *R. sphaeroides* (*29*), and in the model proposed for the W active site of AOR from *P. furiosus* (*30*).

The signal attributed to species IV with axial symmetry was an unexpected result. The *g*-values and relaxation behavior are also compatible with those of an iron−sulfur cluster. However, the detection by EPR and Mösbauer studies of two iron−sulfur clusters of the [4Fe-4S] type in the same ratio excludes this possibility. Further EPR studies performed on *D. desulfuricans* FDH (reference *7* and our unpublished results) showed that overlapped with the already described signals there is a signal that has some features similar to the ones observed for species IV. Also, a similar signal attributed to Mo(V) was observed in the formate- and dithionite-treated samples of *E. coli* FDH ($g_{\|} = 2.094$, $g_{\perp} \sim 2.0$) (*8*). A possible explanation for species IV in *D. gigas* FDH is the existence of two forms of the tungsten sites. One form is described by signal III. The other one, also coordinated to two MGD molecules, has an extra ligand that produces a *g*-shift (signal IV). In the absence of Se, the S of a cysteine is a possible candidate. Nonhomogeneous tungsten sites have been observed in active states of some W-containing proteins (*2*). The significance of these nonhomogeneities is not known.

Our results indicate that *D. gigas* FDH is not related to the best-characterized tungstoproteins which are of the AOR type (*2*). On the other hand, *D. gigas* FDH seems to be related to the Mo-containing FDHs from *D. desulfuricans* (*7*, *10*) *D. vulgaris* (*15*), and *E. coli* (*6*). *E. coli* FDH has the Mo linked to two MGD cofactors and one [4Fe-4S] cluster, while the related *D. desulfuricans* and *D. vulgaris* proteins have in addition a [4Fe-4S] cluster and a third subunit with four hemes *c*. The results obtained for *D. gigas* FDH suggest a tungsten atom coordinated by two MGDs. At present, all the Mo-containing proteins having this type of metal coordination whose structures have been determined contain a similar folding around the metal site (*3*). An interesting question is whether all the proteins containing two MGD cofactors have the same folding regardless of the metal ion.

Remarkably, FDH and ADH from *D. gigas* (*16*) incorporate tungsten in an organism that typically uses molybdenum. The growth medium was not depleted of molybdenum for obtaining *D. gigas* FDH, and from the same crude extract, an AOR which is a Mo-containing enzyme was purified and crystallized (*31*). So it is clear that even with Mo available *D. gigas* FDH prefers to incorporate tungsten. This is not the case for the W-containing *D. gigas* ADH that is only induced when the growth medium is molybdenum-depleted and supplemented with tungsten (*16*). It has been suggested that all the W-containing AOR have a common ancestral AOR-type subunit containing the W−dipterin site and a single [4Fe-4S] cluster (*2*). It seems not to be the case for the *D. gigas* FDH. Our present hypothesis is that likely the *Desulfovibrio* organisms were able at the beginning of their evolution of utilizing both tungsten and molybdenum, expressing now preferably Mo-containing proteins in detriment of the W ones. The presence of a new Mo-containing protein of the AOR type inhibited the expression of the W-ADH. On the other hand, the finding of two closely related FDHs in *Desulfovibrio* organisms, one with tungsten and another with molybdenum, suggests that likely along evolution tungsten was replaced by molybdenum in the *D. desulfuricans* FDH. As seen above, we are studying a homologous FDH from the SRB *D. alaskensis*. Surprisingly,

this protein can incorporate simultaneously molybdenum and tungsten. This result constitutes additional evidence for our hypothesis.

This work describes the characterization of the first W-containing FDH isolated from a SRB and proposes a novel tungsten binding motif with two MGD cofactors. Further work is in progress to elucidate the unusual relaxation behavior as well as the variability of coordination of the W-site as proposed.

ACKNOWLEDGMENT

C.D.B. thanks FOMEC-UNL (Argentina) for financial support for his stay in Portugal. We thank Prof. B. H. Huynh for his friendship and continuous interest in the project, for supporting the ^{57}Fe cell growth, and for allowing us to collect the Mössbauer data in his lab, and R. Toci at the fermentation plant in CNRS (Marseille) for the growth of the cells used in this study.

SUPPORTING INFORMATION AVAILABLE

Polyacrylamide slab gel electrophoresis of *D. gigas* FDH, and pH dependence of *D. gigas* FDH activity (3 pages). This material is available free of charge via the Internet at http://pubs.acs.org.

REFERENCES

1. Hille, R. (1996**)** *Chem. Rev. 96*, 2757−2816.
2. Johnson, M. K., Rees, D. C., and Adams, M. W. W. (1996) *Chem. Rev. 96*, 2817−2839.
3. Romão, M. J., Knäblein, J., Huber, R., and Moura, J. J. G. (1997) *Prog. Biophys. Mol. Biol. 68*, 121−144.
4. Kletzin, A., and Adams, M. W. W. (1996*) FEMS Microbiol. Rev. 18*, 5−63.
5. Mukund, S., and Adams, M. W. W. (1996) *J. Bacteriol. 178*, 163.
6. Boyington, J. C., Gladyshev, V. N., Khangulov, S. V., Stadtman, T. C., and Sun, P. D. (1997) *Science 275*, 1305−1308.
7. Costa, C., Teixeira, M., LeGall, J., Moura, J. J. G., and Moura, I. (1997) *JBIC 2*, 198−208.
8. Khangulov, S. V., Gladyshev, V. N., Dismukes, G. C., and Stadtman, T. C. (1998) *Biochemistry 37*, 3518−3528.
9. George, G. N., Colangelo, C. M., Dong, J., Scott, R. A., Khangulov, S. V., Gladyshev, V. N., and Stadtman, T. C. (1998) *J. Am. Chem. Soc. 120*, 1267−1273.
10. George, G. N., Costa, C., Moura, J. J. G., and Moura, I. (1999) *J. Am. Chem. Soc. 121*, 2625−2626.
11. Ljungdahl, L. G. (1980) in *Molybdenum and Molybdenum-Containing Enzymes* (Coughlan, M. P., Ed.) p 1993, Pergamon Press, New York.
12. Adams, M. W. W., and Mortenson, L. E. (1985) in *Molybdenum Enzymes* (Spiro, T. G., Ed.) p 519, John Wiley, New York.
13. Yamamoto, I., Saiki, T., Liu, S., and Ljungdahl, L. G. (1983) *J. Biol. Chem. 258*, 1826−1832.
14. Deaton, J. C., Solomon, E. I., Watt, G. D., Wetherbee, P. J., and Durfor, C. N. (1987) *Biochem. Biophys. Res. Commun. 149*, 424−430.
15. Sebban, C., Blanchard, L., Bruschi, M., and Guerlesquin, F. (1995) *FEMS Microbiol. Lett. 133*, 143−149.
16. Hensgens, C. M. H., Hagen, W. R., and Hansen, T. H. (1995) *J. Bacteriol. 177*, 6195−6200.
17. Riederer-Henderson, M. A., and Peck, H. D., Jr. (1986) *Can. J. Microbiol. 32*, 430−435.
18. LeGall, J., Mazza, G., and Dragoni, N. (1965) *Biochim. Biophys. Acta 99*, 385−387.
19. Bradford, M. M. (1976) *Anal. Biochem. 72*, 248−254.
20. Lowry, O. H., Rosenbrough, N. J., Farr, A. L., and Randall, R. J. (1951) *J. Biol. Chem. 193*, 265−273.
21. Gremer, L., and Meyer, O. (1996) *Eur. J. Biochem. 238*, 862−866. Frunzke, K., Heiss, B., Meyer, O., and Zumft, W. G. (1993) *FEMS Micobiol. Lett. 113*, 241−246.
22. Liu, C. L., and Mortenson, L. E. (1994) *J. Bacteriol. 159*, 375−380.
23. Dias, J. M., Than, M. E., Humm, A., Huber, R., Bourenkov, G. P., Bartunik, H. D., Bursakov, S., Calvete, J., Caldeira, J., Carneiro, C., Moura, J. J. G., Moura, I., and Romão, M. J. (1999) *Structure 7*, 65−77.
24. Huynh, B. H., Moura, J. J. G., Moura, I., Kent, T. A., LeGall, J., Xavier, A. V., and Münk, E. (1980) *J. Biol. Chem. 255*, 3242−3244.
25. Prince, R. C., Liu, C., Morgan, T. V., and Mortenson, L. E. (1985) *FEBS Lett. 189*, 263−266.
26. Rupp, H., Rao, K. K., Hall, D. O., and Cammack, R. (1978) *Biochim. Biophys. Acta 537*, 255−269.
27. Hirchs, D. J., Beck, W. F., Innes, J. B., and Brudvig, G. W. (1992) *Biochemistry 31*, 532−541.
28. Barnard, K. R., Gable, R. W., and Wedd, A. G. (1997) *JBIC 2*, 623−633.
29. Schindelin, H., Kisker, C., Hilton, J., Rajagopalan, K. V., and Rees, D. C. (1996) *Science 272*, 1615−1621.
30. Koehler, B. P., Mukund, S., Conover, R. C., Dhawan, I. K., Roy, R., Adams, M. W. W., and Johnson, M. K. (1996) *J. Am. Chem. Soc. 118*, 12391−12405.
31. Romão, M. J., Archer, M., Moura, I., Moura, J. J. G., LeGall, J., Engh, R., Schneider, M., Hof, P., and Huber, R. (1995) *Science 167*, 1170−1176.

BI990069N